This document is the Accepted Manuscript version of a Published Work that appeared in final form in : Chemical Communications 2022, https://doi.org/10.1039/D1CC07027D

COMMUNICATION

Copper(I) activation of C–X bonds: Bimolecular vs unimolecular reaction mechanism.

Guillermo Marcos-Ayuso[a], Agustí Lledós,*[b] and Juan A. Casares*[a]

Received 00th January 20xx,
Accepted 00th January 20xx

DOI: 10.1039/x0xx00000x

The oxidative addition of aryl iodides and bromides to [Cu(NHC)R] follows different paths and leads to different products. Two molecules of [Cu(NHC)R] are involved in the addition of aryl iodides, while just one of them participates in the reaction with aryl bromides.

Activation of C–X bonds (X = halogen or pseudo halogen) is an essential step in many catalytic systems. Tricoordinate and tetracoordinated copper(I) complexes can activate C–X bonds by different mechanisms: oxidative addition (concerted or S_N2), homolytic cleavage, or metathesis, and all of them are well represented in copper chemistry.[1-6] Linear copper(I) complexes with NHC ligands also efficiently activate C–X bonds in several catalytic processes, such as the cross-coupling of aryl and allyl halides with aryls or the carbonylative coupling of alkyl halides.[7-9] However there are no mechanistic studies about the Ar–X activation by linear Cu(I) complexes, despite its interest as a comparison term for oxidative addition processes to linear complexes of palladium(0) or gold(I). Because of this, we have started the study of linear copper complexes in copper mediated C–X activation reactions. We have tested the cross-coupling reactions of [Cu(NHC)R] (R = Pf = C_6F_5, or R = Rf = 3,5-dichloro-2,4,6-trifluorobenzene, NHC = DPI = 1,3-Diphenylimidazolium, or NHC = IPr = 1,3-Bis-(2,6-diisopropylphenyl)imidazolinium) with allyl and aryl halides.

The reaction of [Cu(NHC)(Pf)] with allyl chlorides or bromides and with benzilbromide yield the expected cross-coupling product (Pf–allyl or Pf–Bz), however, when allyl iodide is used the metathesis products, [Cu(NHC)(allyl)] and Pf–I, are obtained. The reaction with allyl iodide is too fast to allow its study by NMR, but fortunately similar selectivity, although with slower kinetics, was observed for fluorinated aryls: For Rf–Br as oxidant Rf–Pf, the cross-coupling product, is formed while when Rf–I is used the reaction yields Pf–I and [Cu(NHC)(Rf)] as only products (Scheme 1).

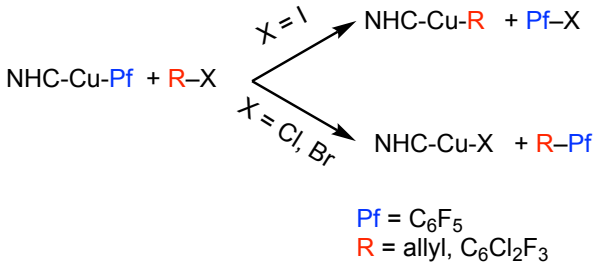

Scheme 1. Observed reaction products of [Cu(NHC)(Pf)] complexes with allyl and fluoroaryl halides.

The metathesis reaction between the complex [Cu(NHC)(Pf)] and Rf–I can be easily monitored by ^{19}F NMR. These two fluoroaryl rings (Pf and Rf) are almost identical in terms of their reactivity, thus the reaction can be considered a *quasi*-self-exchange system, simplifying the kinetic treatment of data.[10,11] The kinetic study of the system showed that the reaction rate is first order on Rf–I and second order on [Cu(DPI)(Pf)] (**1–Pf**), and lead to a value of $\Delta G^{\ddagger}_{298}$= 19.9 kcal mol^{-1} for the reaction. This is a quite anomalous dependence on the metal for a C–E activation, although is not unprecedent in other organometallic reactions: the participation of two monomeric units of the organometallic complex in a catalytic step has been found in Cu-catalyzed azide–alkyne cycloaddition reactions (click chemistry) and attributed to the side-on coordination of the alkyne to copper previous to its reaction with a second copper complex.[12-14] Although the possibility of a termolecular reactions is not negligible,[15] a sensible proposal should explore first bimolecular pathways, which means association of two of the three reagents previous to the rds. Copper(I) organometallics have the ability to produce oligomers in solution,[16] and on the other hand it could be also possible the coordination of Rf–I to the 14e$^-$ [Cu(DPI)(Pf)] (**1–Pf**) before its reaction with a second copper unit. These equilibria may be reached very fast in solution precluding the individual observation of "[Cu(DPI)(Pf)]$_n$" or {[Cu(DPI)(Pf)],I–Rf} species. The measurement of diffusion rates in solution can shed light on the

[a] IU CINQUIMA/Química Inorgánica, Facultad de Ciencias, Universidad de Valladolid, 47011-Valladolid (Spain).e-mail: juanangel.casares@uva.es
[b] Departament de Química, Edifici C.n. Universitat Autònoma de Barcelona, 08193 Cerdanyola del Vallès, Catalonia, Spain.e-mail: agusti.lledos@uab.cat

† Electronic Supplementary Information (ESI) available: Synthesis and full characterisation of the complexes, Kinetic and computational details and extended description of the computational results; 84 pages. See DOI: 10.1039/x0xx00000x

hypothetical association of reagents, because in a fast exchanging system the observed diffusion is an average of the diffusion rates of the components involved in the equilibrium. Both logarithmic and exponential representations of D (D = Diffusion coefficient) vs ln of molecular weight (ln(Mw)) produce linear representations in which the average Mw of the mixture can be read.[17-19] We have previously found that the measurement of diffusion rates by ^{19}F NMR of copper and palladium complexes with fluoroaryl ligands provides linear representations of molecular weight versus D.[11] Applying this methodology we have obtained the data shown in Figure 1 (details in ESI †).

Blue dots represent the experimental values obtained with standard complexes and organic molecules, including pure samples of Rf–I and Pf–I in DMF solution. Colored lines correspond to the ln(D) values obtained for the unknown substances and the ln(Mw) with which they correlate. The diffusion coefficient obtained for [Cu(DPI)(Pf)] (deep blue lines "d" in Figure 1) correlates very well with the Mw of the complex (Calcd. Mw = 481.89, ln(Mw_{calcd}) = 6.18), indicating that there is no self-association in dimers or oligomers species such {[Cu(DPI)(Pf)]$_n$} in a significant amount in solution. Orange line labeled as "g" represent the experimental value of ln(D) of Rf–I when measured in the presence of a threefold excess of [Cu(DPI)(Pf)] (ln(D) = -21.26) which correlates with the value of ln(Mw) = 6.66 (Mw = 783). That means that, in the presence of [Cu(DPI)(Pf)], the diffusion of Rf–I is that of a cluster {[Cu(DPI)(Pf)],Rf–I} (Mw_{calcd} = 777.75). This indicates that there is an association between both reagents forming an assembly that exists in a kinetically relevant concentration. This cluster can react with a second molecule of [Cu(DPI)(Pf)] to activate the

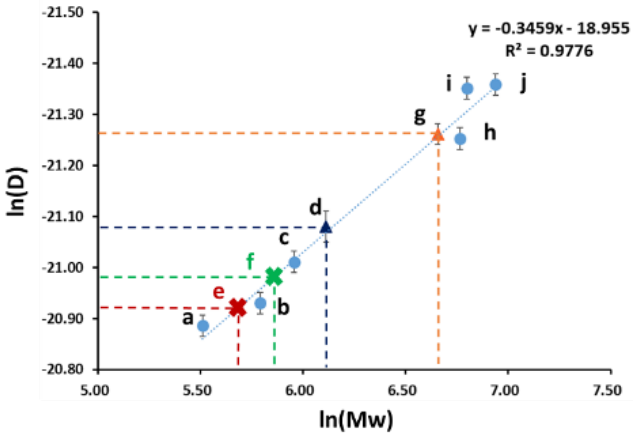

Figure 1. Plot of ln(D) versus ln(Mw). Blue dots represent experimental values obtained for known complexes for the calibration line. Labelled dots correspond to the compounds or mixtures: a = Pf–Br; b = Rf–I; c = [Cu(bipy)(Pf)]; d = [Cu(DPI)(Pf)]; e = [Cu(DPI)(Pf)] + Pf-Br ; f = [Cu(bipy)(Pf] + Rf-I; g = [Cu(DPI)Pf] + Rf-I; h = *cis*–[PdCl(Rf)(PPh_3)$_2$]; i = *cis*–[PdCl(Rf)(dppf)] (dppf =1,1'-Bis(diphenylphosphino)ferrocene), and j = *trans*–[Pd(Rf)$_2$(PPh_3)$_2$] (see ESI† for data of concentration, and other experimental details).

C–I bond. The large change in the ^{19}F NMR chemical shift of Pf–I when measured under a large excess of [Cu(DPI)(Pf)] further supports this association.

To understand the reasons governing the formation of the Pf–I product, we performed a DFT study of the reaction (B3LYP-D3 calculations in N,N-dimethylformamide (DMF) SMD solvent, see details in the Supporting Information). With Rf–I as a substrate we first considered the usual oxidative addition (OA) / reductive elimination (RE) mechanism involving only one [Cu(DPI)(Pf)] complex. Two different pathways arise from the two possible orientations of the Rf–I when approaching [Cu(DPI)(Pf)]. In this way the OA step can yield either a Cu(III) intermediate with Rf and Pf rings mutually *cis* (***I2***$_{cis}$, after crossing ***TSOA1***$_{cis}$, Figure 2a) or a Cu(III) intermediate with Rf and Pf rings mutually *trans* (***I2***$_{trans}$, after crossing ***TSOA1***$_{trans}$, Figure 2b). The *cis*-Pf–Rf intermediate ***I2***$_{cis}$ is ready to form the Rf–Pf product in the RE step, while the *trans*-Pf–Rf intermediate ***I2***$_{trans}$ gives the Pf–I coupling product.

An important conclusion from this initial study is that it does not account for the experimental observation of the Pf–I product. The barrier of the rate-determining OA step is significantly lower in the *cis* pathway, leading to Rf–Pf coupling, than in the *trans* pathway, yielding the experimentally observed Pf–I product (23.9 *vs.* 26.6 kcal mol^{-1}, respectively, Figure 2).

Inclusion in the computed system of a second [Cu(DPI)(Pf)] molecule substantially decreases both the OA and RE barriers of the *trans* pathway, which are reduced to 19.9 and 9.1 kcal mol^{-1}, respectively (Figure 3). The effect on the *cis* pathway is much smaller, the OA barrier being now 22.0 kcal mol^{-1} (see ESI†). Importantly, the presence of the additional [Cu(DPI)(Pf)] molecule reconciles computation with experiment, making *trans* pathway the favored one, with a barrier matching the experimental $\Delta G^{\ddagger}_{298}$ (19.9 kcal mol^{-1}).

Comparing Figures 2b and 3 it can be appreciated that the decrease in the barriers of the *trans* pathway is due to the stabilization of transition states. Intermediates are very little affected by the second copper center. The intermediate ***I12***$_{trans}$ consists of the adduct {[Cu(DPI)(Pf)],Rf–I} in which the iodide has a loose interaction to Cu(2) atom, with a relatively long Cu(2)–I distance of 3.33 Å (see the calculated structure in ESI†). The copper complex has barely deformed its linear structure: the angle C-Cu(2)-C is 173˚. This interaction explains the association between [Cu(DPI)(Pf)] and Rf–I that has been detected in the NMR diffusion experiments. Intramolecular interactions between Au–Cl bonds and distal fluorinated aryls in linear gold(I) [AuCl(L)] complexes (L = fluorinated PR_2(biaryl) phosphines) have been recently characterized.[20] These weak interactions between linear gold(I) complexes and soft donor ligands do not change substantially the geometry at the gold center, while stabilizing the overall structure and have been conceptualized as dipolar interactions. The interaction between the Cu(2) center and the very polarizable iodine atom in the iodoarene in intermediates ***I12***$_{trans}$ and ***I32***$_{trans}$ can be explained using this model.

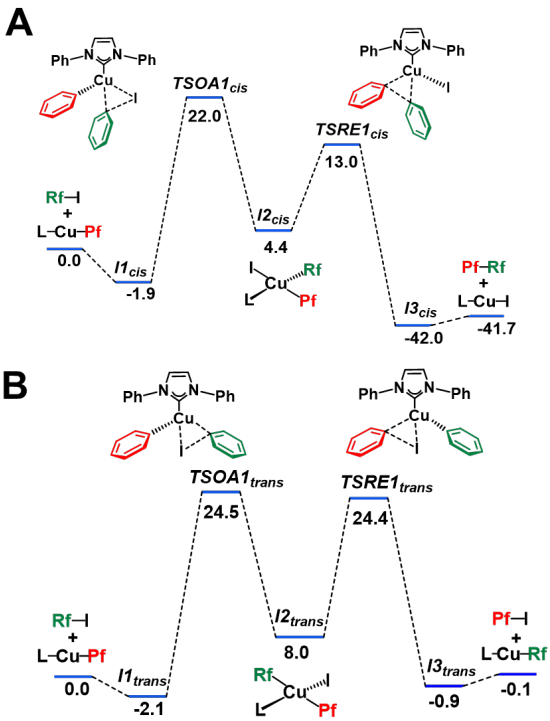

Figure 2. Calculated Gibbs energy profiles (kcal mol^{-1}) for the reaction between [Cu(DPI)(Pf)] (**1-Pf**) and Rf–I (**3**). (a) *Cis* Rf–Pf pathway; (b) *trans* Rf–Pf pathway. Color code: red aryl = C_6F_5; green aryl = 3,5-$C_6F_3Cl_2$. (DFT at B3LYP-D3/BS2 level, SMD solvent model (DMF), 298K).

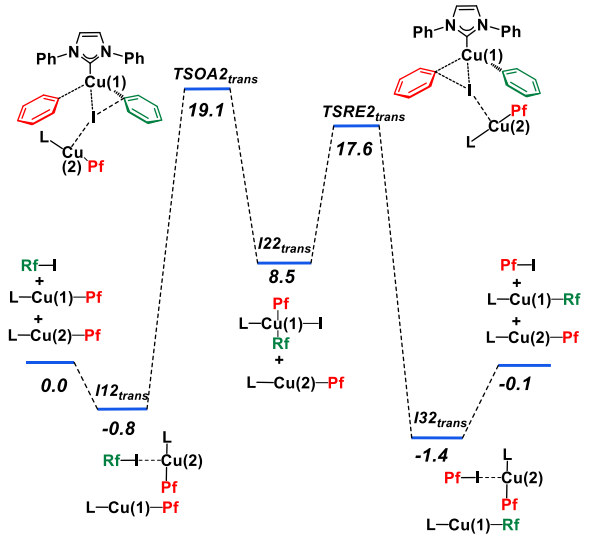

Figure 3. Calculated Gibbs energy profiles (kcal mol^{-1}) for the reaction between [Cu(DPI)(Pf)] (**1-Pf**) and Rf-I (**3**) in presence of a second [Cu(DPI)(Pf)] molecule to produce the aryl metathesis (*trans* pathway). Color code: red aryl = C_6F_5; green aryl = 3,5-$C_6F_3Cl_2$. (DFT at B3LYP-D3/BS2 level, SMD solvent model (DMF), 298K).

The presence of a second [Cu(DPI)(Pf)] molecule also modifies significantly the geometry of the oxidative addition transition sate (compare ***TSOA1***$_{trans}$ and ***TSOA2***$_{trans}$ in Figure 4). Moreover, Cu(2) –I distance has notably shortened to 2.97 Å in ***TSOA2***$_{trans}$ (Figure 4), suggesting the existence of a bonding interaction between the iodide and Cu(2) as the origin of its stabilization. The Cu(2)–I Wiberg index (0.23) agrees with the existence of such interaction. The surprising stability of the ***TSOA2***$_{trans}$ compared to ***TSOA1***$_{trans}$ can be understood using NBO analysis. Remarkably, significant donation from a (LP)I NBO orbital (55% s 45%p) to an empty (LP*) Cu(2) NBO orbital (100% p), involving a second order perturbation energy of 22 kcal mol^{-1} was identified in ***TSOA2***$_{trans}$**.** These values also suggest that the Cu(2) complex stabilizes the electron density that evolves at the iodine during the oxidative addition of Cu(1) to the C–I bond.

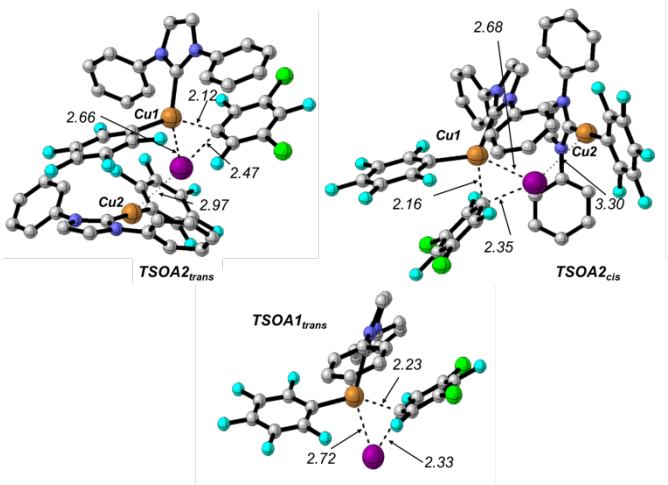

Figure 4. Calculated geometries for **TSOA2**$_{trans}$, **TSOA2**$_{cis}$ and **TSOA1**$_{trans}$. Selected distances in Å. 3D-structures were generated using CYLview. [21]

The copper labelled as Cu(1) interacts with both the carbon ipso of the fluoroaryl and the iodine in a concerted addition, and its geometry is close to square-planar. The stereochemistry leading to the *trans* disposition of the two aryls in Cu(I) is controlled by the bulkiness of the carbene attached to Cu(2). In the transition state of the *cis* rearrangement (***TSOA2***$_{cis}$, Figure 4) the DPI ligand interacts with the same ligand in Cu(1), precluding a closer approach. As a consequence, in ***TSOA2***$_{cis}$ the Cu(2)–I distance remains at almost the same value than in ***I12***$_{cis}$ (3.30 and 3.36 Å, respectively). In this way there is not a strengthened Cu(2)–I interaction in the TS and the barrier for the OA in the *cis* pathway is similar with or without the additional [Cu(DPI)(Pf)] molecule (22.0 and 23.8 kcal mol^{-1}, respectively, see Figure 2 and Figure S13 for the Gibbs energy profiles of the *cis* pathway). The Cu(2) –I interaction in the OA transition state of the *trans* pathway places its energy below that of the *cis* pathway. The same analysis holds for the RE step: *trans* RE transition state is even more stabilized than *trans* OA transition state for the interaction with Cu(2) unit (RE barrier decreased from 16.4 in ***TSRE1***$_{trans}$ to 9.1 in ***TSRE2***$_{trans}$, Figure 2b and 3). Cu(2)–I diminishes from 4.35 Å in ***I22***$_{trans}$ to 2.87 Å in ***TSRE2***$_{trans}$. Thus, Cu(2)–I interaction in the transition sates is modifying the stereochemistry of the addition, favoring the formation of the aryl metathesis product.

The stabilization of transition states by a second copper does not operates with other halides as bromide or chloride because of the very week interaction of these halides with copper(I) that does not compensate the loss of entropy of the association {complex,X–R}. In fact, the measurement of diffusion rates of Rf–Br in the presence of [Cu(DPI)(Pf)] shows that there is not association of these two compounds (see dark-red line labeled "e" in Figure 3) thus the oxidative addition takes place in a bimolecular mode, first order on [Cu(DPI)(Pf)] accordingly to its kinetic reaction order. Calculations agree with this behavior: there is no stabilization of OA and RE transition states of the reaction with Rf–Br. For the OA step the barriers are 33.4 kcal mol^{-1} with one [Cu(DPI)(Pf)] molecule and 36.7 with an additional [Cu(DPI)(Pf)] molecule (see ESI†). The incipient Br^- in the OA addition is not interacting with Cu(2) (distance Cu(2)–Br = 3.95 Å in ***Br–TSOA2$_{trans}$***).

The diffusion coefficient of Rf–I is not affected either by the presence of [Cu(bipy)(Pf)], which is consistent with the observation of a first order rater law in copper observed for the oxidative addition of these reagents. This is probably due to the low acidity of a trigonal-planar Cu complex when compared with a linear 14e– NHC derivative. Therefore, it seems that the association of halides with copper complexes is a peculiar characteristic of iodides and that it occurs preferentially on 14e– copper complexes.

Activation of the Ar–I bond by linear copper complexes occurs through the interaction of two copper atoms with aryl iodide. This mode of activation does not require the formation of a copper dimer, on the contrary, it is based on the prior formation of a cluster of aryl iodide with a copper complex in kinetically relevant concentration, which has been detected experimentally. This group reacts with a second copper complex, on which oxidative addition occurs. The stabilization is efficient in the transition states of the C–I breaking and forming bonds, which is where the iodine atom has an increased I^- character. The weak interaction between $14e^-$ copper complexes and the iodine of organic substrates leads to the breaking and forming of the C–I bond assisted by two copper complexes (Scheme 2). The stabilization of the transition state can be attributed to the stabilization of the charge of the iodine by the second copper. The operation of this mechanisms has a dramatic change in the course of the reaction: since it leads to the *trans*-[CuI(NHC)(Pf)(Rf)] instead of the *cis*, no cross-coupling products are formed, but the metathesis of the halogen is produced instead.

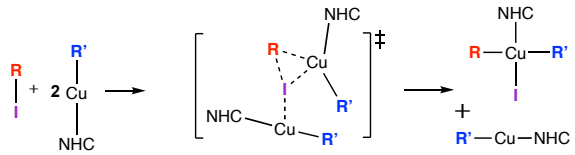

Scheme 2. Bimolecular C–X activation.

The weak association of other halogens to copper prevents them from taking this reaction pathway, leading to a classical oxidant addition followed by C–C elimination.

The authors thank the Spanish MCIN (projects PID2019-111406GB-I00 and PID2020-116861GB-I00) and the Junta de Castilla y León (project VA224P20), for financial support.

Conflicts of interest

There are no conflicts to declare

Notes and references

1 G. O. Jones, P. Liu, K. N. Houk, and S. L. Buchwald, *J. Am. Chem. Soc.* 2010, ***132***, 6205-6213.
2 E. D. Kalkman, M. G. Mormino, and J. F. Hartwig, *J. Am. Chem. Soc.* 2019, ***141***, 19458-19465.
3 O. Lozano-Lavilla, P. Gómez-Orellana, A. Lledós, and J. A. Casares, *Inorg. Chem.* 2021, ***60***, 11633-11639.
4 R. Giri, A. Brusoe, K. Troshin, J. Y. Wang, M. Font, and J. F. Hartwig, *J. Am. Chem. Soc.* 2018, ***140***, 793-805.
5 A. J. Clark, *Eur. J. Org. Chem.* 2016, ***2016***, 2231-2243.
6 J. M. Muñoz-Molina, T. R. Belderrain, and P. J. Pérez, *Eur. J. Inorg. Chem.* **2011**, 3155–3164.
7 W. Xie, and S. Chang, *Angew. Chem. Int. Ed.* 2016, ***55***, 1876–1880.
8 D. Li, X.-X. Wu, T. Gao, B. Li, and S. Chen, *Org. & Biomol. Chem.* 2017, ***15***, 7282-7285.
9 L.-J Cheng, N. P. Mankad, *Acc. Chem. Res*. 2021, **54**, 2261-2274.
10 M. Pérez-Iglesias, R. Infante, J. Casares, and P. Espinet, *Organometallics* 2019, ***38***, 3688-3695.
11 M. Pérez-Iglesias, O. Lozano-Lavilla, and J. A. Casares, *Organometallics,* 2019, ***38***, 739-742.
12 C. Nolte, P. Mayer, and B. F. Straub, *Angew. Chem. Int. Ed.* 2007, ***46***, 2101-2103.
13 (a) V. O. Rodionov, V. V. Fokin., M. G. Finn, *Angew Chem Int. Ed.* 2005, **44**, 2210-2215. (b) S. I. Presolski, V. Hong, S.-H. Cho, and M. G. Finn, *J. Am. Chem. Soc.* 2010, ***132***, 14570–14576.
14 L. Jin, D. R. Tolentino, M. Melaimi, G. Bertrand, Jin, L.; *Sci. Adv.* 2015, ***1***, e1500304.
15 G. Lente, *Curr. Opin. Chem. Eng.* 2018, ***21***, 76-83.
16 G. van Koten, *Organometallics*. 2012, ***26***, 7634-7646, and references therein.
17 R. Neufeld, and D. Stalke, *Chem. Sci.* 2015, ***6***, 3354-3364.
18 C. S. Johnson Jr., *Prog. Nuc. Magn. Res. Spec.* 1999, ***34***, 203-256.
19 G. Dal Poggetto, V. U. Antunes, M. Nilsson, G. A. Morris, and C. F. Tormena, *Magn. Reson. Chem.* 2017, ***55***, 323-328.
20 J. Ponce-de-León, R. Infante, M. Pérez-Iglesias, and P. Espinet *Inorg. Chem.* 2020, ***59***, 16599-16610.
21 CYLview, 1.0b; Legault, C. Y. Université de Sherbrooke, 2020 (http://www.cylview.org)